

The impact of ENSO and the NAO on extreme winter precipitation in North America in observations and regional climate models

Kirien Whan¹ · Francis Zwiers¹

Received: 11 September 2015 / Accepted: 23 April 2016 / Published online: 27 May 2016
© The Author(s) 2016. This article is published with open access at Springerlink.com

Abstract The relationship between winter precipitation in North America and indices of the North Atlantic Oscillation (NAO) and El Niño–Southern Oscillation (ENSO) is evaluated using non-stationary generalized extreme value distributions with the indices as covariates. Both covariates have a statistically significant influence on precipitation that is well simulated by two regional climate models (RCMs), CanRCM4 and CRCM5. The observed influence of the NAO on extreme precipitation is largest in eastern North America, with the likelihood of a negative phase extreme rainfall event decreased in the north and increased in the south under the positive phase of the NAO. This pattern is generally well simulated by the RCMs although there are some differences in the extent of influence, particularly south of the Great Lakes. A La Niña-magnitude extreme event is more likely to occur under El Niño conditions in California and the southern United States, and less likely in most of Canada and a region south of the Great Lakes. This broad pattern is also simulated well by the RCMs but they do not capture the increased likelihood in California. In some places the extreme precipitation response in the RCMs to external forcing from a covariate is of the opposite sign, despite use of the same lateral boundary conditions and dynamical core. This demonstrates the importance of model physics for teleconnections to extreme precipitation.

Keywords Extreme precipitation · GEV · ENSO · NAO

1 Introduction

The observed relationships between mean and extreme precipitation with large-scale modes of variability have been extensively studied. Given that regional climate models (RCMs) are the primary source of high-resolution climate projections, evaluation of the simulation of extreme precipitation events that are associated with these large-scale modes is necessary. It is important to understand if and where the mechanisms associated with extreme events are simulated correctly, so that we can be confident that models simulate the statistics of extreme events for the right reasons. Two major modes of climate variability that influence North America are El Niño–Southern Oscillation (ENSO) and the North Atlantic Oscillation (NAO). Both modes are characterized by two phases that have differing impacts on North American precipitation.

El Niño is the warm phase of ENSO and La Niña is the cool phase. La Niña is a strengthening of the mean state of the tropical Pacific, with cooler sea-surface temperature (SST) anomalies in the east and a stronger than normal Walker Circulation. During El Niño warm SST anomalies are found in the tropical eastern Pacific, which are associated with a weakening or reversal of tropical trade winds and shifts in the jet stream (Ning and Bradley 2014a). The significant influence of ENSO on mean precipitation in North America has been well-established. ENSO has an influence on mean and extreme precipitation in western and southern North America, primarily in winter and spring (Ropelewski and Halpert 1986; Kenyon and Hegerl 2010; Zhang et al. 2010; Schubert et al. 2008; L’Heureux et al. 2015). Regionally, El Niño is associated with reduced cool-season precipitation (Shabbar et al. 1997) and stream flow (Bonsal and Shabbar 2008) from western Canada to the Great Lakes. In the southwestern United States, El Niño

✉ Kirien Whan
kwhan@uvic.ca

¹ The Pacific Climate Impacts Consortium, University of Victoria, University House 1, Stn CSC, PO Box 1700, Victoria, BC V8W 2Y2, Canada

is associated with positive precipitation anomalies (Schonher and Nicholson 1989; L'Heureux et al. 2015). In eastern North America El Niño is associated with precipitation increases along the coast and negative anomalies over the Ohio Valley and into southeastern Canada (Ning and Bradley 2014b), with a similar pattern found for moderate indices of extreme precipitation (Ning and Bradley 2014a).

The NAO is the major large-scale mode of atmospheric variability over the extra-tropical Atlantic Ocean. It is characterized by a meridional dipole of sea-level pressure (SLP) anomalies between high and subtropical latitudes over the Atlantic Ocean. The positive phase of the NAO is associated with a weakening of the Icelandic low and a strengthening of the subtropical Azores high-pressure system that results in an enhanced pressure gradient, a stronger jet stream and a strengthening of the westerlies (Portis et al. 2001; Archambault et al. 2008). In the negative phase there are weakened westerlies associated with a reduced pressure gradient (Hurrell 1995; Archambault et al. 2008). These changes in circulation influence the climate of eastern North America (Ning and Bradley 2014b; Archambault et al. 2008). The positive phase of the NAO is associated with increased precipitation frequency and positive daily rainfall anomalies in the northeastern United States (Durkee et al. 2007; Archambault et al. 2008) while in northern and eastern Canada there is reduced precipitation and stream flow (Ning and Bradley 2014b; Bonsal and Shabbar 2008). The precipitation response is the opposite during the negative phase, with a shift towards less frequent precipitation in the northeastern United States (Archambault et al. 2008) and increased precipitation in eastern Canada (Bonsal and Shabbar 2008). Differences in SLP between positive and negative phase NAO years align well with precipitation differences, with a boundary between increases and decreases around 40°N, as higher pressure blocks winter storm activity (Ning and Bradley 2014b). The NAO is also associated with changes in indices of extreme precipitation in eastern North America, with a similar pattern of increased precipitation in the north and decreases in the south (Ning and Bradley 2014a). Furthermore, extreme daily precipitation anomalies (defined as daily anomalies greater than two standard deviations from the mean) are more likely in the northeastern United States during the positive phase (Archambault et al. 2008).

The relationships of ENSO and the NAO with moderate indices of extreme precipitation are reasonably well-established but fewer studies have examined the relationship of these teleconnections to statistically extreme events using an extreme value theory framework. Zhang et al. (2010) quantified the influence of the NAO and ENSO on extreme winter precipitation using non-stationary generalized extreme value (GEV) distributions with indices of ENSO and the NAO as covariates. In a station-based

analysis they found no significant influence of the NAO on extreme North American winter precipitation (Zhang et al. 2010). The influence of ENSO was significant, with up to a four times increase in the probability of extreme events in the southern United States (Zhang et al. 2010). Consistent with these results is the increased waiting times for a 1-in-20 year event under La Niña for the Gulf of Mexico and the east coast of the United States (Schubert et al. 2008).

We do not expect a limited area model will improve on large-scales that exceed the computational domain (Diaconescu and Laprise 2013) but an improvement in the simulation of extremes, particularly rainfall, is generally assumed. Examination of teleconnections between features occurring outside the RCM domain and simulated precipitation in the current climate is a critical question that has received limited attention, particularly given the need for confidence in high-resolution climate projections that are used for planning and adaption purposes. It is necessary to assess not only whether an RCM simulates the statistics of climate extremes correctly (Whan and Zwiers 2015; Martynov et al. 2013 provide such evaluations for the CanRCM4 and CRCM5) but also to evaluate whether the models simulate the teleconnections with large-scale climate features well (Whan et al. 2015b). The study of RCMs simulation of 'moderate' indices of climate extremes has been extensive. Previous work has shown that generally CanRCM4 and CRCM5 simulate extreme precipitation well, although both models tend to over-estimate climatological mean precipitation with the largest wet biases found in CRCM5 (Whan and Zwiers 2015).

The issue of whether climate models can correctly simulate relationships between large-scale climate features and extreme events has received considerably less attention than evaluation of the statistics of extremes, although several regional studies are worth noting. It has been demonstrated that the evaluation runs of NARCCAP-generation RCMs (that use lateral boundary conditions derived from reanalysis products) are able to reproduce the ENSO-related mean precipitation features in the western United States (Leung et al. 2003). Compared to several stations located in the southwestern United States, the evaluation simulations of NARCCAP RCMs were generally able to capture the direction and magnitude of the correlation between precipitation and the SOI. Further, a RCM (RCA version 3, Samuelsson et al. 2011) forced with reanalysis boundary conditions demonstrated that the regional model is able to capture the seasonal mean precipitation anomalies in the tropical Americas that are associated with ENSO forcing, as well as the variability between ENSO events (Tourigny and Jones 2009). For the northeast United States, a reanalysis driven RCM (SUNYA RCM, which is based on MM5) is generally able to reproduce the precipitation in the northeast United States associated with the La Niña event of November

1998–March 1999, although there were some discrepancies in the location and magnitude of the maximum precipitation (Notaro et al. 2006). While these studies have been limited to only one RCM they demonstrate the ability of regional models to simulate variations in mean precipitation associated with ENSO. The impacts of the NAO teleconnection in RCMs has received less attention for North America, however Previdi and Veron (2005) demonstrate that an ensemble of the Polar MM5 forced with a reanalysis product over Greenland and northeast Canada was able to reproduce the reduced precipitation over Greenland and the Labrador Sea during positive NAO months.

In this study we consider the relationship between statistically extreme precipitation events and large-scale modes of climate variability. First we extend the work of Zhang et al. (2010) using gridded observed precipitation and a high-resolution reanalysis product. The second novel aspect of this study is an evaluation of the ability of the two Canadian RCMs (CanRCM4 and CRCM5) to simulate the observed relationships between extreme precipitation and the NAO and ENSO using a non-stationary GEV framework.

2 Data and methods

2.1 Data

We focus on the monthly maxima of daily precipitation from an extended winter period (November–December–January–February, NDJF) from 1989–2009. This extended cool-season is chosen for analysis because it is a period when the influence of ENSO is large (Rasmusson and Carpenter 1982) and it covers most of the winter period when the NAO influence is strong (Hurrell 1995).

We compare two observationally-based data sets, ANUSPLIN + Livneh and the North American Regional Reanalysis (NARR, Mesinger et al. 2006, with two RCMs (CanRCM4 and CRCM5). ANUSPLIN + Livneh is based directly on station observations in Canada (McKenney et al. 2011) and the continental United States (Livneh et al. 2013), which are combined with bilinear interpolation at the border; see Whan and Zwiers (2015) for more information on this data set. We classify NARR as ‘observationally-based’ as it assimilates precipitation observations over North America, although this assimilation finishes in 2003 for Canada (Rapaic et al. 2015). Despite this assimilation caution is required when interpreting precipitation from reanalysis products and so we include an evaluation of NARR compared to ANUSPLIN + Livneh before discussing the RCMs. In the absence of a daily gridded continent-wide observational product some compromise must be made, so while combining the two observed products at the

Table 1 Information about the data sets used in this study, including the original horizontal resolution (degrees), the use of spectral nudging for scales larger than 2000 km and the source in each data set

Name	Original resolution	Spectral nudging	Institute
CanRCM4_0.44	0.44	Yes	CCCma
CanRCM4_0.22	0.22	Yes	CCCma
CanRCM4_NS	0.44	No	CCCma
CanRCM4_SNNS	0.44	Yes/no	CCCma
CRCM5_0.44	0.44	No	UQAM
CRCM5_0.22	0.22	No	UQAM
NARR	0.33	NA	CFS + UoW
ANUSPLIN + Livneh	0.08	NA	NCEP

Acronyms for the institutes: *CCCma* The Canadian Centre for Climate Modelling and Analysis, *UQAM* L’Université du Québec à Montréal, *CFS* The Canadian Forest Service, *NCEP* The National Centers for Environmental Prediction, *UoW* The University of Washington

border and the use of reanalysis product as ‘observations’ is not ideal, our results show that it is reasonable in this case.

The observational products are compared to two RCMs (Table 1), CanRCM4 (Scinocca et al. 2015) and CRCM5 (Zadra et al. 2008). A detailed description of the model set ups can be found in Whan et al. (2015b) and Whan and Zwiers (2015) but a brief description is also included here. Both of these Canadian RCMs were run as part of the COordinated Regional climate Downscaling EXperiment (CORDEX) experiment (Giorgi et al. 2009) over North America. They use lateral boundary conditions from ERA-Interim Reanalysis (Dee et al. 2011), including sea-surface temperatures. They have the same dynamical core from the Global Environmental Multiscale (GEM) numerical prediction model (Cote et al. 1998) but use different nesting strategies and physics schemes. The CanRCM4 simulations use spectral nudging (except for CanRCM4_NS), the physics packages from the global model (CanESM2) and the Canadian Land Surface Scheme (CLASS, Verseghy 2000) Version 2.7 (Verseghy 1991; Verseghy et al. 1993) land surface scheme (Scinocca et al. 2015). In this study, CRCM5 is run without spectral nudging, uses parameterizations from the GEM model and uses CLASS Version 3.5 for the land surface scheme (Verseghy 2011; Zadra et al. 2008). For both models we use the 0.44° (CanRCM4_0.44, CanRCM4_NS and CRCM5_0.44) and 0.22° (CanRCM4_0.22 and CRCM5_0.22) simulations. Pre-processing of all data sets included the removal of ocean based points (where required) and interpolation to the CanRCM4 0.44° rotated-pole grid using bilinear interpolation from the Climate Data Operators (The Max Planck Institute for Meteorology 2013). While all CORDEX generation models use the same rotated-pole grid, the original dimensions of CRCM5 and

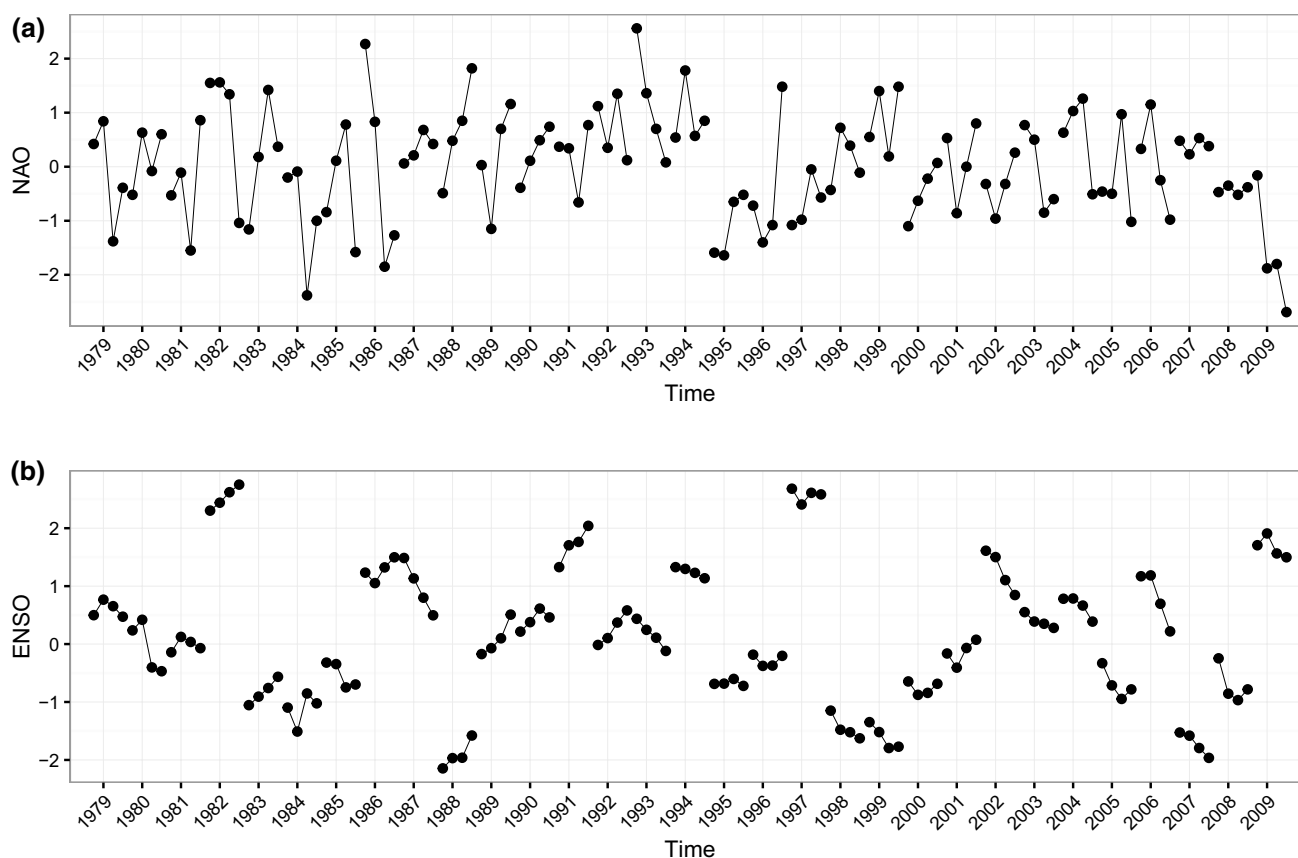


Fig. 1 The standardized monthly anomalies of **a** the NAO index and **b** the Niño 3.4 index in winter (November–February, omitting the remaining months). These indices are used as covariates in the non-stationary GEV analysis

the higher resolution simulations are larger than the final CanRCM4 0.44° grid. We restrict the analysis to Canada and the continental United States to match the extent of the ANUSPLIN + Livneh data set.

Indices of ENSO and the NAO are used as covariates in the GEV analysis. The Niño 3.4 index is the area averaged standardized SST anomalies from the tropical Pacific (5° N–5°S, 170°W–120°W) from the HadISST data set (Rayner et al. 2003). The NAO index is based on normalized sea-level pressures between the Azores Islands and Iceland (Hurrell 1995), and is downloaded from the Climatic Research Unit of the University of East Anglia (<http://www.cru.uea.ac.uk/cru/data/nao/>). The monthly winter time series of both indices can be seen in Fig. 1.

2.2 Methods

The GEV distribution can be described by three parameters and is used to model block maxima (Coles 2001). The parameters of the GEV are the location (μ), the scale (σ) and the shape (ξ). Under idealized conditions, as the size of the block grows without bound the data fits one of the

following distributions, depending on ξ ; Gumbel if $\xi = 0$, the Frechet if $\xi > 0$ or the Weibull if $\xi < 0$.

The GEV distribution was fitted to NDJF precipitation without covariates in the stationary case (M0). The use of 1-month blocks results in four block maxima per year and a final sample size of 80 block maxima over the 20-year study period. There are some assumptions in this method that are worth mentioning. The use of short blocks is relatively common in climate studies (Zhang et al. 2010; Sillmann et al. 2011; Whan et al. 2015a) but assumes that a month of observations is long enough for the distribution of maxima to be well approximated by the GEV. Fitting the GEV via maximum likelihood further assumes that there is no relationship between maxima in different months (apart from the possible influence of the covariates, as discussed below). Also, the use of several maxima from the same year assumes that they all have the same statistical distribution with little influence of the annual cycle. The r -largest method fits the GEV to the r -largest values per block. Larger values of r may be preferred from a data inclusion perspective but may also violate the asymptotic support for the extreme value distributions. Previous climate studies

Table 2 The lag-1 autocorrelation of monthly winter block maxima with the influence of (a) NAO and (b) ENSO removed

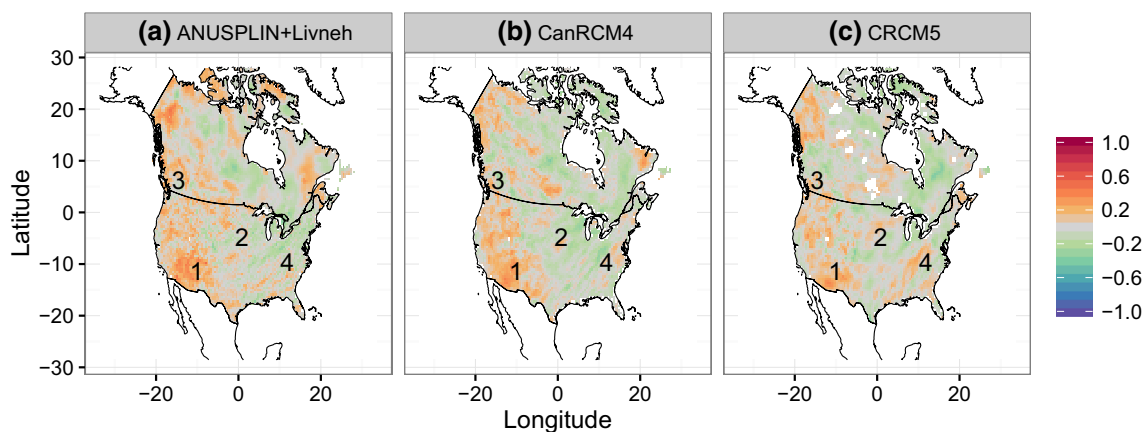
	(a) NAO	(b) ENSO
ANUSPLIN + Livneh	9.59	8.77
NARR	11.29	10.97
CanRCM4_0.44	8.05	7.12
CanRCM4_0.22	7.11	5.81
CanRCM4noSN	5.74	5.45
CRCM5_0.44	4.82	5.84
CRCM5_0.22	6.37	6.19

have used $r = 3$ (Zhang et al. 2010). To assess the relationship between maxima in different months we examine the percentage of pixels where the lag-1 auto-correlation is significant (at the 5 % significance level, relative to white noise), after removing the influence of the covariates (Table 2). We find the autocorrelation is significant at between 4.82 and 11.29 % of pixels, predominately located in the south-west (Fig. 2). This suggests the violation of the independence assumption in some locations and these pixels are where most failed goodness-of-fit tests are located (see discussion of the goodness-of-fit test below and spatial patterns in Figs. 4 and 5). It should be noted that serial correlation in the underlying data series and amongst the block maximum does not indicate that the GEV distribution is inappropriate for describing the asymptotic properties of the block maxima. The underlying limit theory that predicts that the distributions of block maxima converge to the GEV distribution as block length increases holds for stationary processes with a range of dependence characteristics (e.g., see Leadbetter et al. 1983). For all such processes, we would expect block maxima to become independent as block lengths increase without limit. Detection of serial

correlation at some locations hints that blocks remain relatively short, which is corroborated by the goodness-of-fit test results in these locations since they indicate discernible differences between the distributions of the block maxima and the expected asymptotic GEV distribution. Visual inspection of model and empirical quantiles at several locations throughout the domain indicates a reasonable fit with few deviations that would suggest the violation of these assumptions at these representative locations (Fig. 3).

In the non-stationary cases we assess the influence of the NAO and ENSO by fitting models with a covariate (z , NAO index or Niño 3.4) on either the location parameter only (M1) or on both the location and scale parameters (M2). Where a covariate is included on the location parameter, it varies linearly with the covariate so that $\mu(z) = \beta_0 + \beta_1 z$. Where a covariate is included on the scale parameter, it is allowed to vary log-linearly with the covariate to ensure the scale parameter remains positive, so that $\log(\sigma) = \gamma_0 + \gamma_1 z$ (Zhang et al. 2010). The fit of the GEV to winter precipitation in North America is tested with the application of a standard Kolmogorov–Smirnov (KS) goodness-of-fit test to M2 after transformation to a standard Gumbel distribution, using the significance level $p < 0.05$.

The likelihood-ratio test is used to evaluate the significance of increasing model complexity by introducing covariates (Zhang et al. 2010). Selection of M1 and M2 as the best model indicates that the inclusion of the covariate on the location parameter (M1) or both the location and scale parameters (M2) significantly improved the model fit compared to M0 and M1, respectively. We calculate the significance of the covariate on North American precipitation by finding the percentage of pixels where M1 or M2 are selected as the best model and compare it to the 5 % significance level that is expected by chance. However the issue of multiple testing arises when a field of individual

**Fig. 2** Spatial patterns of the lag-1 autocorrelation in **a** ANUSPLIN + Livneh, **b** CanRCM4_0.44 and **c** CRCM5_0.44. Numbers indicate the points in Fig. 3 from 1 south-west North America, 2 central North America, 3 British Columbia and 4 south-east North America

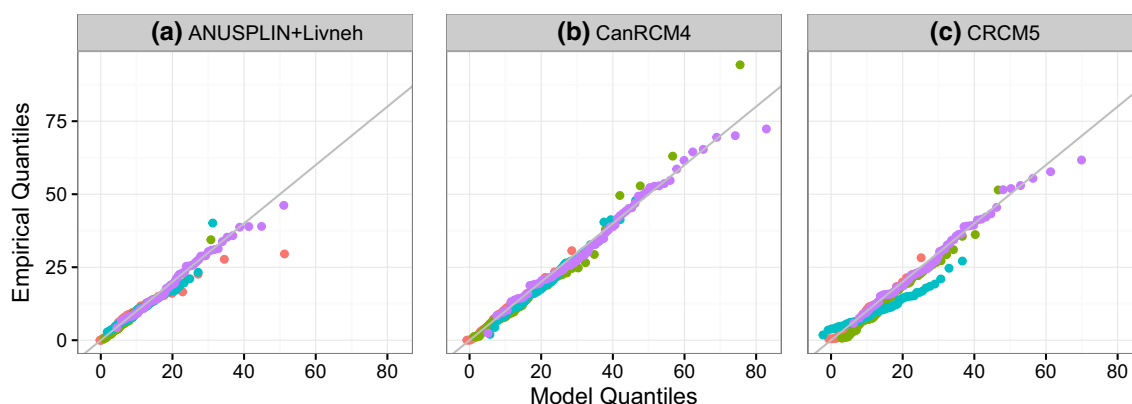


Fig. 3 Example quantile–quantile plots from three points showing model and empirical quantiles for **a** ANUSPLIN + Livneh, **b** CanRCM4_0.44 and **c** CRCM5_0.44. Quantiles are calculated from sim-

ulated precipitation in at points in south-west North America (purple), the central North America (green), British Columbia (pink), and south-east North America (blue). See Fig. 2 for point locations

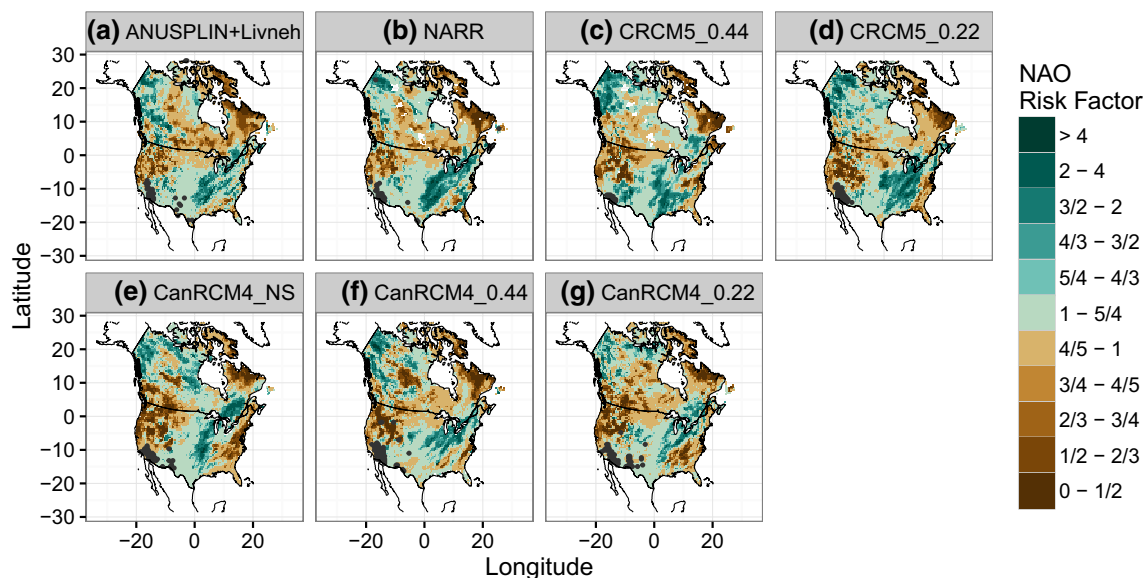


Fig. 4 The observed and simulated NAO risk factor in **a** ANUSPLIN + Livneh, **b** NARR, **c** CRCM5_0.44, **d** CRCM5_0.22, **e** CanRCM4_NS, **f** CanRCM4_0.44 and **g** CanRCM4_0.22. Pixels where

the GEV is not a good-fit for monthly maximum precipitation are marked by dark grey dots

significance tests are evaluated simultaneously, so we also assess the global significance of the results. Traditional approaches to assess field significance are often based on a count of the number of local significance tests that reject the null hypothesis (Livezey and Chen 1983). One shortcoming of these approaches is that they ignore the results of the local test, i.e. the p values themselves. An alternative method is based on the false discovery rate (FDR), which is the expected proportion of falsely rejected null hypotheses from the set of local tests (Renard et al. 2008; Wilks 2006; Ventura et al. 2004). The FDR can be controlled at a global significance level ($\alpha = 0.05$) and a FDR probability

is defined for each p value in the set of K ordered p values, $p_{(1)} \dots p_{(k)}$, where $p_{(1)}$ is the smallest p value, by:

$$P_{FDR} = \max_{j=1, \dots, k} [p_{(j)} : p_{(j)} \leq \alpha(j/K)]. \quad (1)$$

Field significance is declared at the α significance level if at least one local null hypothesis has a p -value less than the P_{FDR} and is thus rejected at the global significance level (Renard et al. 2008; Wilks 2006). The FDR method assumes that all tests are independent, which is generally not true for spatial climate data, but Wilks (2006) showed that the method is robust to spatial dependence (Renard

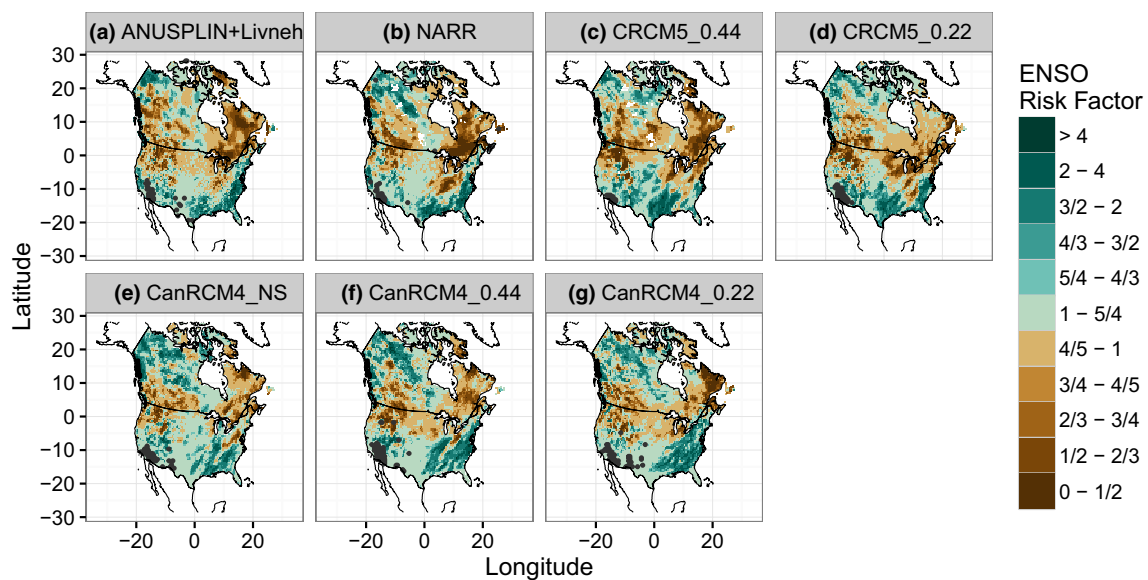


Fig. 5 The observed and simulated ENSO risk factor in **a** ANUSPLIN + Livneh, **b** NARR, **c** CRCM5_0.44, **d** CRCM5_0.22, **e** CanRCM4_NS, **f** CanRCM4_0.44 and **g** CanRCM4_0.22. Pixels where

the GEV is not a good-fit for monthly maximum precipitation are marked by dark grey dots

et al. 2008; Wilks 2006). Field significance is achieved for all results presented below.

We evaluate the influence of spectral nudging by concatenating two simulations that differ only in their nesting strategy, CanRCM4_0.44 (uses spectral nudging) and CanRCM4_NS (no spectral nudging). In this model, M3, we fit two covariates on the location parameter, (1) the index of either the NAO or Niño 3.4 as in M1 and (2) a binary variable with 0 for spectral nudging and 1 for no spectral nudging. This method allows the influence of spectral nudging to be quantified through a likelihood ratio test comparing M1 with M3.

Finally, the influence of each covariate is expressed through a ‘risk factor’. We calculate the effective 20-year return value (20RV) under the negative phase of the covariate at each pixel. To be consistent with Zhang et al. (2010) we characterize the negative phase as the 5th smallest value and the positive phase as the 5th largest value. The risk factor is the expected change in the probability of the negative phase 20RV occurring under the positive phase of each covariate, expressed as a scaling factor (Zhang et al. 2010).

All analysis is conducted in the R Statistical Computing environment (R Development Core Team 2014) and the GEV analysis uses the ‘extRemes’ package (Gilleland 2014).

3 Results and discussion

For each mode of variability, we first compare the influence of the covariates on North American extreme precipitation

in NARR and ANUSPLIN + Livneh, before discussing how well these observed teleconnections are simulated by the RCMs.

3.1 NAO

The influence of the NAO on extreme precipitation in ANUSPLIN + Livneh and NARR is similar, as the NAO significantly improves model fit at 11.6 and 12.5 % of pixels, respectively (Table 3). Consistent with the current understanding of NAO impacts (Ning and Bradley 2014b), the strongest contrast between phases of the NAO is found in eastern North America (Fig. 4a, b). In northeastern Canada an extreme rainfall event that occurs once in 20-years under the negative phase of the NAO is less than half as

Table 3 Percentage of local significant tests where a non-stationary model was selected as the best fit, with confidence intervals in parentheses

	NAO	ENSO
ANUSPLIN + Livneh	11.57 (10.84–12.33)	12.38 (11.63–13.16)
NARR	12.50 (11.74–13.31)	14.63 (13.81–15.49)
CanRCM4_0.44	10.29 (09.58–11.04)	12.68 (11.90–13.50)
CanRCM4_0.22	11.32 (10.59–12.08)	10.04 (09.35–10.77)
CanRCM4_NS	13.53 (12.73–14.37)	12.32 (11.55–13.12)
CRCM5_0.44	11.23 (10.49–12.01)	13.36 (12.56–14.20)
CRCM5_0.22	11.38 (10.67–12.14)	12.91 (12.15–13.71)

Confidence intervals are estimated from the binomial distribution

likely to occur under the positive phase. In the region south of the Great Lakes, the NAO risk factor is between 2 and 4, meaning that a negative phase NAO extreme rainfall event is up to four times more likely under the positive phase. This dipole pattern in north and south eastern North America is consistent with previous studies (Ning and Bradley 2014b; Durkee et al. 2007; Bonsal and Shabbar 2008). The spatial pattern of NAO influence is generally comparable between the two observationally-based data sets, although the magnitude of increased likelihood of negative NAO extreme precipitation under a positive NAO regime is somewhat larger in the central and eastern United States in NARR compared to ANUSPLIN + Livneh (Fig. 4). This comparison demonstrates that the significant influence of the NAO on extreme precipitation is comparable in NARR and ANUSPLIN + Livneh and well above the level expected by chance, suggesting that the NAO has a significant influence on North American extreme precipitation, even in these short data sets (Table 3). Previous work using a station-based data set over the period 1949–2003 and the months December–March found that the NAO failed to achieve field significance for North America as there was a significant influence at fewer than 8 % of stations (Zhang et al. 2010). We attribute this difference to two factors. First, we define winter as the November–February period and we find a somewhat smaller percentage of pixels with a significant influence if we use the December–March period (i.e. for ANUSPLIN + Livneh there is a significant influence at 8.7 % of pixels). Secondly, and most importantly, there is an area of significant influence in northeast Canada that is not captured by an analysis of station data due to the sparse observing network. Confidence in the robustness of this result depends on confidence in ANUSPLIN and NARR's representation of precipitation in northeastern Canada, which may be low given the sparse observational network (Rapaic et al. 2015). However NARR captures the spatial variability of total precipitation in the Canadian Arctic well, despite a wet bias since the end of observed precipitation assimilation in 2003. For the eastern Canadian Arctic specifically, total precipitation in NARR is not significantly different than observations in January–February–March but has a wet bias in October–November–December (Rapaic et al. 2015). We are reasonably confident in this result given the positive evaluation of Arctic precipitation in NARR (Rapaic et al. 2015) and the similarity between NARR and ANUSPLIN (Fig. 4).

The extent of NAO influence in the RCMs is comparable to observations, with a significant influence of between 10.3 and 13.5 % of North America in the CanRCM4 and CRCM5 simulations. The magnitude of the NAO risk factors in the CanRCM4 and CRCM5 simulations (Fig. 4c–g) are smaller in central and eastern US compared to NARR (Fig. 4b) but more similar in magnitude

to ANUSPLIN + Livneh (Fig. 4a). Both RCMs simulate a region in the south-east United States where the estimated likelihood of a negative phase NAO extreme event is decreased under the positive phase, that is too extensive compared to both ANUSPLIN + Livneh and NARR. The extent of the region south of the Great Lakes where the positive phase of the NAO increases the likelihood of a negative phase extreme event is reduced in CanRCM4 simulations and CRCM5_0.44 and over-estimated in CRCM5_0.22. As a result there are some regions where the RCMs simulate an extreme precipitation response to the NAO that is of the opposite sign, despite the use of the same lateral boundary conditions.

The influence of spectral nudging of the large-scales on the NAO teleconnection is small (Fig. 4e, f). There are some differences in the spatial pattern of the NAO risk factor in the two 0.44° CanRCM4 simulations that are run with (CanRCM4_0.44) and without (CanRCM4_NS) spectral nudging. There is a region in the northeast United States where a negative NAO precipitation event in CanRCM4_NS is less likely under the positive phase of the NAO, which is inconsistent with CanRCM4_0.44 (Fig. 4f) and observations (Fig. 4a, b). A similar inconsistency, but of the opposite sign, is evident in southeast Canada where CanRCM4_NS has a positive risk factor while CanRCM4_0.44, ANUSPLIN + Livneh and NARR are negative. However the CRCM5 simulations do not use any spectral nudging and CRCM5_0.22 simulates a NAO risk factor of the same sign as CanRCM4 and observations in these areas. Comparison of the models that included (M3) and did not include (M1) a covariate indicator for spectral nudging in the concatenated CanRCM4 simulations (CanRCM4_SNNs) gives an indication of whether the spectral nudging has an influence on extreme precipitation. The result is field significance as the smallest p-value satisfies the condition in Eq. 1. However, the result is not robust given that only one local significance test remains significant after adjusting for the FDR. In addition, only 4.88 % of pixels see an improvement when a second covariate is included in the model, which is very close to the 5 % improvement rate expected by chance. Overall the result does not provide robust evidence that spectral nudging influences extreme precipitation after controlling for the influence of the NAO.

3.2 ENSO

The extent of influence of ENSO on extreme precipitation is similar in ANUSPLIN + Livneh and NARR, as ENSO has a significant influence at 12.4 and 14.6 % of pixels from M2, respectively (Table 3). The conditions for field significance are met and the number of local significance tests that reject the null hypothesis is far above the expected number. However the percentage of significant local tests is smaller

than the 22 % of stations that had a significant influence of ENSO the station-based analysis, likely due to a smaller sample size (80 values per pixel here compared with 220 per station in Zhang et al. 2010). A La Niña extreme rainfall event is 2–4 times more likely to occur under El Niño in California and the southeast United States (Fig. 5a, b), consistent with Zhang et al. (2010). In the Pacific Northwest and most of Canada (excluding northwest Canada) El Niño is associated with a decrease in the probability of a La Niña magnitude extreme event (Shabbar et al. 1997; Bonsal and Shabbar 2008). The region of decreased ENSO risk factor extends south into the western and eastern United States, with the likelihood of a La Niña extreme rainfall event decreased under El Niño in the areas north and south of the Great Lakes (Fig. 5a, b). There are some small differences between the ENSO risk factors of ANUSPLIN + Livneh and NARR, including the region of negative risk factor south of the Great Lakes that is larger (more negative) in NARR compared to ANUSPLIN + Livneh, the change of sign between small negative and positive risk factors in the northern central US and the extensive region of large positive risk factor in northeastern Canada in NARR that is not evident in ANUSPLIN + Livneh. Overall the extreme rainfall response to ENSO is similar in ANUSPLIN + Livneh and NARR, despite these small differences (Fig. 5a, b).

In both observationally-based data sets there is a sharp delineation at the eastern US-Canadian border between increased and decreased likelihood of an extreme once in 20 years La Niña event occurring under El Niño (Fig. 5a, b). This feature is evident in the previous NAO risk factors and in a station-based analysis, although the coarse 5° gridding of the ENSO risk factor in the previous work likely minimizes the border effects (Zhang et al. 2010). The pattern is also evident in the third EOF of monthly precipitation that is associated with ENSO (see Fig. 1 from Ning and Bradley 2014b).

The extent of ENSO influence in the CanRCM4 and CRCM5 simulations is comparable to the observationally-based data sets, with between 10 and 13.4 % of local significance tests passing at the 0.05 level and field significance is declared for all simulations. The influence of ENSO on CanRCM4_0.22 extreme precipitation is significant after controlling for the FDR but not robust as the p values of only two local significance tests are below P_{FDR} .

Generally the RCMs capture the spatial pattern of the ENSO teleconnection to extreme rainfall events in North America, but there are some regional discrepancies that are worth noting (Fig. 5c–g). Neither model simulates the observed large increased probability of a La Niña extreme rainfall event under El Niño conditions in California, regardless of horizontal resolution or nesting strategy (Fig. 5). Furthermore, the ENSO response in the northeastern United States varies between the CanRCM4 and

CRCM5 simulations despite use of the same lateral boundary conditions and dynamical core, demonstrating the importance of model physics for the ENSO teleconnection to extreme winter rainfall. In this region, the CanRCM4 simulations capture the increased likelihood of a La Niña extreme event under El Niño conditions best compared to observations, while the sign of the relationship is opposite for this region in CRCM5.

In the area south of the Great Lakes the CRCM5 simulations are more similar to observations, as a once in 20-years La Niña precipitation event is estimated to be less likely under El Niño conditions. The CanRCM4 simulations have an extensive region of increased likelihood under El Niño stretching from Florida to the Great Lakes which is not evident in observations and can be seen in the simulations with and without spectral nudging (Fig. 5e, f). Again, the result is not robust as only one local significance test satisfies the conditions of the FDR test for field significance (Eq. 1). The influence of spectral nudging on extreme precipitation in CanRCM4_SNNS may be significant but is likely small, with very close to 5 % of local significance tests rejecting the null hypothesis (4.67 %).

4 Conclusions

We first evaluated the influence of the NAO and ENSO in two observationally-based data sets, ANUSPLIN + Livneh and NARR over the period 1989–2009 using non-stationary generalized extreme value distributions. Both modes of variability significantly improve model fit, demonstrating the significant influence of the NAO and ENSO on extreme winter precipitation on the continental scale. The spatial patterns of the changed probability of a negative phase extreme event under the positive phase of the covariate were broadly similar, although there were some fine scale differences.

We find that the NAO has a significant influence on North American precipitation, contrary to a previous station-based analysis (Zhang et al. 2010). This difference is likely due to the inclusion of more information from northeastern Canada in the gridded data sets that are not available for a station-based analysis. Although the spatial pattern of NARR precipitation in the Canadian Arctic has been shown to match observations (Rapačić et al. 2015) and the result is consistent with the influence of the NAO (Archambault et al. 2008), caution should be employed when interpreting this result in such a data poor region. The influence of the NAO on observed extreme precipitation is largest in eastern North America. In northeast Canada the likelihood of a precipitation event that would occur once every 20-years under the negative phase of the NAO is decreased when the NAO is positive, consistent with the

decreased precipitation and stream flow that is associated with the positive phase of the NAO (Bonsal and Shabbar 2008; Archambault et al. 2008). The NAO has the opposite influence in the eastern United States, with the likelihood of a negative phase extreme event increased when the NAO is positive, in agreement with previous work (Durkee et al. 2007; Archambault et al. 2008). The spatial pattern and magnitude of the NAO teleconnection is broadly captured by the RCMs, although the extent of this region in the eastern United States is under-estimated by CanRCM4 and over-estimated by CRCM5, with some regions of the opposite sign in the two RCMs.

ENSO has a significant influence on extreme winter precipitation in all data sets. The influence of ENSO on extreme precipitation events is largest in southern and western North America. In California and the southeast United States the likelihood of a La Niña extreme precipitation event is increased under El Niño conditions. While in the Pacific northwest, eastern Canada and the area south of the Great Lakes, El Niño reduces the probability of a La Niña extreme precipitation event. The RCMs capture the regions in the Pacific Northwest and southeast United States reasonably well but do not simulate an increased probability in California. CanRCM4 captures the observed increased probability of a La Niña extreme precipitation event under El Niño in the northeast United States, while CRCM5 has a decreased probability in this area. The opposite is true in a region south of the Great Lakes where CRCM5 has the same direction response as observations (decreased likelihood under El Niño) but the response in CanRCM4 is of the opposite sign.

The regions where the two RCMs simulate an extreme precipitation response of opposite signs despite use of the same lateral boundary conditions and thus the same large-scale forcing are noteworthy as they demonstrate some regional deficiencies of teleconnections in the RCMs. The differing extreme precipitation response to the same external forcing, from either ENSO or the NAO, adds another layer of uncertainty onto future projections. This is in addition to the uncertainty already associated with the simulation of large-scale modes of climate variability in global climate models, particularly ENSO. We showed that the use of spectral nudging had a limited influence on the simulated teleconnections with extreme winter precipitation. It is likely that many differences are related to differences in the physics schemes used in the two models. Additional work is required to explore further the mechanisms and parameterizations that lead to these differing responses in the RCMs.

Acknowledgments This work is supported by the Canadian Network for Regional Climate and Weather Processes (CNRCWP) and the Pacific Climate Impacts Consortium. CNRCWP is funded by the National Science and Engineering Research Council (NSERC).

ECMWF ERA-Interim data used in this study were obtained from the ECMWF data server. We acknowledge the World Climate Research Programme's Working Group on Regional Climate, and the Working Group on Coupled Modelling, the former coordinating body of CORDEX. Thanks to Alex Cannon for providing the observational data set. We also thank the climate modelling groups (CCCma, UQAM) for producing and making available their model output. We also acknowledge the Earth System Grid Federation infrastructure, an international effort led by the US Department of Energy's Program for Climate Model Diagnosis and Intercomparison, and thank two anonymous reviewers for their constructive comments.

Open Access This article is distributed under the terms of the Creative Commons Attribution 4.0 International License (<http://creativecommons.org/licenses/by/4.0/>), which permits unrestricted use, distribution, and reproduction in any medium, provided you give appropriate credit to the original author(s) and the source, provide a link to the Creative Commons license, and indicate if changes were made.

References

- Archambault HM, Bosart LF, Keyser D, Ayyer AR (2008) Influence of large-scale flow regimes on cool-season precipitation in the northeastern United States. *Mon Weather Rev* 136(8):2945–2963
- Bonsal B, Shabbar A (2008) Impacts of large-scale circulation variability on low streamflows over Canada: a review. *Can Water Resour J* 33(2):137–154
- Coles S (2001) An introduction to statistical modeling of extreme values
- Cote J, Gravel S, Methot A, Patoine A, Roch M, Staniforth A (1998) The operational CMC-MRB global environmental multiscale (GEM) model. Part I: design considerations and formulation. *Mon Weather Rev* 126(6):1373
- Dee DP, Uppala SM, Simmons AJ, Berrisford P, Poli P, Kobayashi S, Andrae U, Balmaseda MA, Balsamo G, Bauer P, Bechtold P, Beljaars ACM, van de Berg L, Bidlot J, Bormann N, Delsol C, Dragani R, Fuentes M, Geer AJ, Haimberger L, Healy SB, Hersbach H, Hólm EV, Isaksen L, Kållberg P, Köhler M, Matricardi M, McNally AP, Monge-Sanz BM, Morcrette J-J, Park B-K, Peubey C, de Rosnay P, Tavolato C, Thépaut J-N, Vitart F (2011) The ERA-Interim reanalysis: configuration and performance of the data assimilation system. *Q J R Meteorol Soc* 137(656):553–597
- Diaconescu EP, Laprise R (2013) Can added value be expected in RCM-simulated large scales? *Clim Dyn* 41(7–8):1769–1800
- Durkee JD, Frye JD, Fuhrmann CM, Lacke MC, Jeong HG, Mote TL (2007) Effects of the North Atlantic oscillation on precipitation-type frequency and distribution in the eastern United States. *Theor Appl Climatol* 94(1–2):51–65
- Gilleland E (2014) extRemes: extreme value analysis
- Giorgi F, Jones C, Asrar G (2009) Addressing climate information needs at the regional level: the CORDEX framework. *WMO Bull* 58(3):175–183
- Hurrell JW (1995) Decadal trends in the North Atlantic oscillation: regional temperatures and precipitation. *Science* 4(269):676–679
- Kenyon J, Hegerl GC (2010) Influence of modes of climate variability on global precipitation extremes. *J Clim* 23(6248–6262):23
- Leadbetter MR, Lindgren G, Rootzen H (1983) Extremes and related properties of random sequences and processes. Springer, New York
- Leung LR, Qian Y, Bian X, Hunt A (2003) Hydroclimate of the western United States based on observations and regional climate

- simulation of 1981–2000. Part II: mesoscale ENSO anomalies. *J Clim* 16(12):1912–1928
- Livezey RE, Chen WY (1983) Statistical field significance and its determination by Monte Carlo techniques. *Mon Weather Rev* 111(1):46–59
- Livneh B, Rosenberg EA, Lin C, Nijssen B, Mishra V, Andreadis KM, Maurer EP, Lettenmaier DP (2013) A long-term hydrologically based dataset of land surface fluxes and states for the conterminous United States: update and extensions*. *J Clim* 26(23):9384–9392
- L'Heureux ML, Tippett MK, Barnston AG (2015) Characterizing ENSO coupled variability and its impact on North American seasonal precipitation and temperature. *J Clim* 28(10):4231–4245
- Martynov A, Laprise R, Sushama L, Winger K, Šeparović L, Dugas B (2013) Reanalysis-driven climate simulation over CORDEX North America domain using the Canadian Regional Climate Model, version 5: model performance evaluation. *Clim Dyn* 41:2973–3005
- McKenney DW, Hutchinson MF, Papadopol P, Lawrence K, Pedlar J, Campbell K, Milewska E, Hopkinson RF, Price D, Owen T (2011) Customized spatial climate models for North America. *Bull Am Meteorol Soc* 92(12):1611–1622
- Mesinger F, DiMego G, Kalnay E, Mitchell K, Shafran PC, Ebisuzaki W, Jović D, Woollen J, Rogers E, Berbery EH, Ek MB, Fan Y, Grumbine R, Higgins W, Li H, Lin Y, Manikin G, Parrish D, Shi W (2006) North American regional reanalysis. *Bull Am Meteorol Soc* 87(3):343–360
- Ning L, Bradley RS (2014a) Winter climate extremes over the northeastern United States and southeastern Canada and teleconnections with large-scale modes of climate variability. *J Clim* 28(6):2475–2493
- Ning L, Bradley RS (2014b) Winter precipitation variability and corresponding teleconnections over the northeastern United States. *J Geophys Res Atmos* 119(13):2014JD021591
- Notaro M, Wang W-C, Gong W (2006) Model and observational analysis of the northeast US regional climate and its relationship to the PNA and NAO patterns during early winter. *Mon Weather Rev* 134(11):3479–3505
- Portis DH, Walsh JE, El Hamly M, Lamb PJ (2001) Seasonality of the North Atlantic oscillation. *J Clim* 14(9):2069–2078
- Previdi M, Veron DE (2005) North Atlantic oscillation-related climate variability in a regional atmospheric model. *J Geophys Res Atmos* 110(D16):D16106
- R Development Core Team (2014) R: a language and environment for statistical computing. R Foundation for Statistical Computing
- Rapačić M, Brown R, Markovic M, Chaumont D (2015) An evaluation of temperature and precipitation surface-based and reanalysis datasets for the Canadian Arctic, 1950–2010. *Atmos Ocean* 53(3):283–303
- Rasmusson EM, Carpenter TH (1982) Variations in tropical sea surface temperature and surface wind fields associated with the Southern Oscillation/El Niño. *Mon Weather Rev* 110(5):354–384
- Rayner NA, Parker D, Horton E, Folland C, Alexander L, Rowell D (2003) Global analyses of sea surface temperature, sea ice, and night marine air temperature since the late nineteenth century. *J Geophys Res* 108:D144407
- Renard B, Lang M, Bois P, Dupeyrat A, Mestre O, Niel H, Sauquet E, Prudhomme C, Parey S, Paquet E, Neppel L, Gailhard J (2008) Regional methods for trend detection: assessing field significance and regional consistency. *Water Resour Res* 44(8):W08419
- Ropelewski CF, Halpert MS (1986) North American precipitation and temperature patterns associated with the El Niño/Southern Oscillation (ENSO). *Mon Weather Rev* 114(12):2352–2362
- Samuelsson P, Jones CG, Willén U, Ullerstig A, Gollvik S, Hansson U, Jansson C, Kjellström E, Nikulin G, Wyser K (2011) The Rossby Centre Regional Climate model RCA3: model description and performance. *Tellus A* 63(1):4–23
- Schonher T, Nicholson SE (1989) The relationship between California rainfall and ENSO events. *J Clim* 2(11):1258–1269
- Schubert SD, Chang Y, Suarez MJ, Pegion PJ (2008) ENSO and wintertime extreme precipitation events over the contiguous United States. *J Clim* 21(1):22–39
- Scinocca J, Kharin VV, Jiao Y, Qian M, Lazare M, Solheim L, Flato G (2015) Coordinated global and regional climate modelling. *J Clim* Submitted
- Shabbar A, Bonsal B, Khandekar M (1997) Canadian precipitation patterns associated with the Southern Oscillation. *J Clim* 10(12):3016–3027
- Sillmann J, Croci-Maspoli M, Kallache M, Katz RW (2011) Extreme cold winter temperatures in Europe under the influence of North Atlantic atmospheric blocking. *J Clim* 24(5899–5913):22
- The Max Planck Institute for Meteorology (2013) CDO: climate data operators
- Tourigny E, Jones CG (2009) An analysis of regional climate model performance over the tropical Americas. Part I: simulating seasonal variability of precipitation associated with ENSO forcing. *Tellus A* 61(3):323–342
- Ventura V, Paciorek CJ, Risbey JS (2004) Controlling the proportion of falsely rejected hypotheses when conducting multiple tests with climatological data. *J Clim* 17(22):4343–4356
- Verseghy D (2011) CLASS: THE CANADIAN LAND SURFACE SCHEME (VERSION 3.5). Technical Documentation (Version 1), Environment Canada, Climate Research Division, Science and Technology Branch, Canada
- Verseghy DL (1991) Class-A Canadian land surface scheme for GCMS. I. Soil model. *Int J Climatol* 11(2):111–133
- Verseghy DL (2000) The Canadian land surface scheme (CLASS): its history and future. *Atmos Ocean* 38(1):1–13
- Verseghy DL, McFarlane NA, Lazare M (1993) Class-A Canadian land surface scheme for GCMS, II. Vegetation model and coupled runs. *Int J Climatol* 13(4):347–370
- Whan K, Zscheischler J, Orth R, Shongwe M, Rahimi M, Asare E, Seneviratne SI (2015a) Impact of soil moisture on extreme maximum temperatures in Europe. *Weather Clim Extremes*
- Whan K, Zwiers FW (2015) Evaluation of extreme rainfall and temperature over North America in CanRCM4 and CRCM5. *Clim Dyn*
- Whan K, Zwiers FW, Sillmann J (2015b) The influence of atmospheric blocking on extreme winter minimum temperatures in North America. *J Clim* (submitted)
- Wilks DS (2006) On “field significance” and the false discovery rate. *J Appl Meteorol Climatol* 45(9):1181–1189
- Zadra A, Caya D, Cote J, Dugas B, Jones C, Laprise R, Winger K, Caron L (2008) The next Canadian regional climate model. *Phys Can* 64(2):75–83
- Zhang X, Wang J, Zwiers FW, Groisman PY (2010) The influence of large-scale climate variability on winter maximum daily precipitation over North America. *J Clim* 23(2902–2915):11